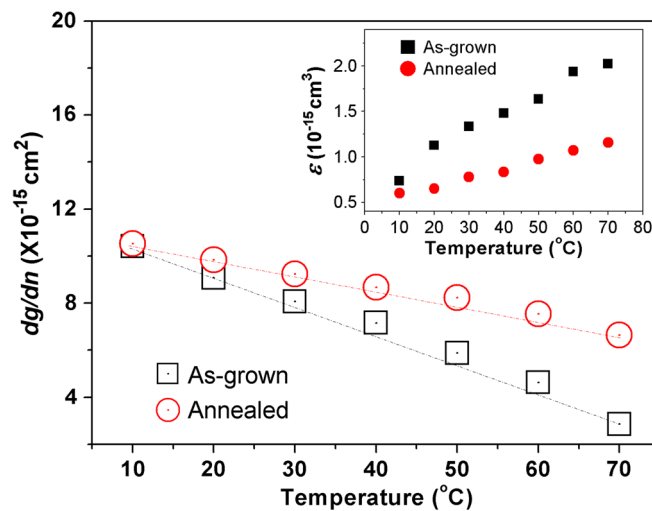


# Effects of Thermal Annealing on the Dynamic Characteristics of InAs/GaAs Quantum Dot Lasers

Volume 2, Number 4, August 2010

H. X. Zhao, Student Member, IEEE  
S. F. Yoon, Senior Member, IEEE  
C. Y. Ngo  
R. Wang, Student Member, IEEE  
C. Z. Tong, Member, IEEE  
C. Y. Liu, Member, IEEE  
Q. Cao



DOI: 10.1109/JPHOT.2010.2052843  
1943-0655/\$26.00 ©2010 IEEE

# Effects of Thermal Annealing on the Dynamic Characteristics of InAs/GaAs Quantum Dot Lasers

H. X. Zhao,<sup>1</sup> *Student Member, IEEE*, S. F. Yoon,<sup>1</sup> *Senior Member, IEEE*,  
C. Y. Ngo,<sup>2</sup> R. Wang,<sup>1</sup> *Student Member, IEEE*, C. Z. Tong,<sup>3</sup> *Member, IEEE*,  
C. Y. Liu,<sup>4</sup> *Member, IEEE*, and Q. Cao<sup>1</sup>

<sup>1</sup>School of Electrical and Electronic Engineering, Nanyang Technological University, Singapore 639798

<sup>2</sup>Patterning and Fabrication Capability Group, Institute of Materials Research and Engineering, Singapore 117602

<sup>3</sup>Edward S. Rogers, Sr. Department of Electrical and Computer Engineering, University of Toronto, Toronto, ON M5S 1A1, Canada

<sup>4</sup>Institut für Festkörperphysik, Technische Universität Berlin, 10623 Berlin, Germany

DOI: 10.1109/JPHOT.2010.2052843  
1943-0655/\$26.00 ©2010 IEEE

Manuscript received May 28, 2010; accepted June 7, 2010. Date of publication June 8, 2010; date of current version June 25, 2010. Corresponding author: H. X. Zhao (e-mail: zhao0097@ntu.edu.sg).

**Abstract:** We investigated the effects of rapid thermal annealing (RTA) on the dynamic characteristics of the InAs/GaAs ten-layer quantum dot (QD) laser. Improvements in the temperature stability of bandwidth have been demonstrated upon annealing. We attribute the improvements to the following factors: 1) increase in internal quantum efficiency and 2) reduction in temperature dependency of differential gain. The increase in bandwidth at high temperature from the annealed QDs could be due to a reduction in the relaxation time on the order of 0.1 ps. More importantly, the RTA process resulted in better temperature stability in the differential gain and gain compression. This is beneficial for the development of uncooled high-speed QD lasers.

**Index Terms:** Quantum dots (QD), semiconductor lasers.

## 1. Introduction

Quantum dot (QD) systems have been studied extensively for high-speed operation of semiconductor lasers. This is because QDs have been proposed to increase the modulation speed as a result of its discrete energy levels and three-dimensional (3-D) carrier confinement. As differential gain is recognized as one of the crucial factors for the modulation speed of the QD laser [1]–[4], the *p*-doping technique was proposed because it increases the differential gain and improves its temperature stability. However, due to the fact that a fraction of the holes provided by the doped barriers reside in the 2-D wetting layer (WL) valance band states [3], [5], the results are disappointing since the differential gain only increases slightly. It is speculated that slow carrier relaxation, which has a direct impact on the differential gain, is one of the factors that limits the modulation speed of QD lasers [2], [6]. In addition, the QDs' stochastic size distribution also limits the differential gain [7], thus limiting the modulation speed of QD lasers.

Postgrowth rapid thermal annealing (RTA) has attracted significant interest since it is an effective method to improve the uniformity of the QDs [8]–[10]. Many had observed at the material level that, upon annealing, there are reduction in the carrier lifetimes of both QD ground-state (GS) and excited-state (ES) [10], as well as shorter photoluminescence (PL) rise time [9], which accounts for carrier transport in the barriers and carrier capture and relaxation in the QDs. On the contrary,

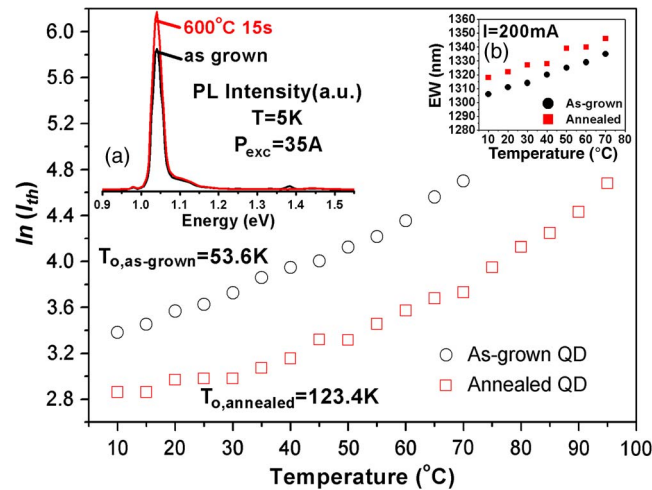


Fig. 1. Plot of  $\ln(I_{th})$  versus temperature for as-grown and annealed lasers with 1 mm cavity length. (a) PL spectra of the as-grown sample and the sample annealed at 600 °C for 15 s measured at 5 K. (b) Temperature-dependent emission wavelength (EW) of the two devices.

reported results at the device level are significantly less. Furthermore, existing works mainly report the static characteristics of annealed QDs [8], [11], [12]. To the best of our knowledge, there exist no works on the investigation of the dynamic characteristics, i.e., differential gain ( $dg/dn$ ) and nonlinear gain compression factor ( $\epsilon$ ), of the annealed QD lasers.

In this paper, we investigate the effects of RTA on the high-speed performance of InAs/GaAs QD lasers. The temperature dependency of internal quantum efficiency, internal loss, differential gain, and nonlinear gain compression factor of the annealed and as-grown 1.3- $\mu\text{m}$  QDs are also studied.

## 2. Experimental Details

The ten-layer self-assembled InAs/GaAs QD laser structure used in this experiment was grown on GaAs (100) substrate by molecular beam epitaxy (MBE). The structure consists of QD active region sandwiched between two 1.5  $\mu\text{m}$  C- and Si-doped  $\text{Al}_{0.35}\text{Ga}_{0.65}\text{As}$  cladding layers. The active layer comprises 2.3 monolayer (ML) of InAs QDs capped by a 5-nm  $\text{In}_{0.15}\text{Ga}_{0.85}\text{As}$  layer. A 33-nm GaAs layer is used to separate the two QD layers [13]. The indium-containing layers were grown at 485 °C, while the (Al)GaAs layers were grown at  $\sim 580$  °C. The QD areal density is around  $5 \times 10^{10} \text{ cm}^{-2}$ . The QD samples were capped with 200 nm of  $\text{SiO}_2$  deposited by plasma-enhanced chemical vapor deposition (PECVD). The annealing process was then performed in  $\text{N}_2$  ambient at 600 °C for 15 s using a rapid thermal processor. Subsequently, the as-grown and annealed samples were processed into 4- $\mu\text{m}$ -wide ridge waveguide (RWG) lasers using pulsed anodic oxidation (PAO) method at room temperature (RT) [14]. The small-signal modulation response of the as-cleaved QD lasers was measured under continuous-wave (CW) biasing condition using a vector network analyzer (VNA) and a high-speed photoreceiver. The measurements have been normalized to the frequency response of the photoreceiver. A thermoelectric temperature controller monitors the device temperature during measurements.

## 3. Results and Discussion

Fig. 1 shows the temperature-dependent threshold current ( $I_{th}$ ) for the as-grown and annealed lasers deduced from the temperature-dependent power-current measurements. Note that the cavity length ( $L$ ) of both the as-grown and annealed laser chips is 1 mm. The characteristic temperatures ( $T_0$ ) for the as-grown and annealed samples are 52.6 K and 123.4 K, respectively. At each temperature, the annealed samples show lower  $I_{th}$  than the as-grown samples. This could be attributed to the removal of grown-in defects upon annealing since these act as non-radiative

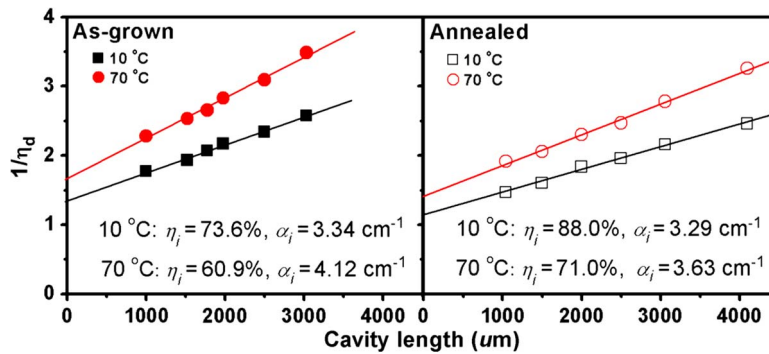


Fig. 2. Plot of inverse external quantum efficiency  $1/\eta_d$  as a function of cavity length for the as-grown and annealed lasers.

recombination centers in the QD [8], [11], [12]. Furthermore, the annealed lasers exhibited lasing up to 95 °C, while the as-grown lasers only lased up to 70 °C. Fig. 1(a) shows the PL spectra for the as-grown and annealed samples measured at 5 K. The significant increase ( $\sim 26\%$ ) in the PL intensity after annealing is due to the sizable reduction in the material defectivity [15], [16], which is related to the diffusion and capture processes in the barrier—this is expected to result in an improvement in the device performance due to the increase in radiative efficiency, as indicated by the improvement of the PL spectra. The center wavelength for the annealed samples was found to remain unchanged as compared with the as-grown ones. This is attributed to the suppression of interdiffusion of indium atom under the strain field within or near QDs due to the relatively large number of stacking [17]. The temperature-dependent emission wavelength (EW) of the lasers at injection current of 200 mA is shown Fig. 1(b). As expected, the wavelength increases with temperature for both the as-grown and annealed lasers. However, notice that the EW of the annealed QD lasers is slightly longer ( $\sim 0.9\%$ ) than that of the as-grown ones for a given temperature, although one does not see such differences in the PL spectra of Fig. 1(a). At this point, it is worth highlighting that, since the threshold current of the annealed lasers is much lower than that of the as-grown ones, higher  $I/I_{th}$  ratio is expected in the annealed samples at a given injection current at each temperature. Therefore, the injected current of 200 mA in this case is 10 times the threshold current of the annealed lasers but only 6.7 times that of the as-grown ones at 10 °C. Consequently, the slight difference in the lasing wavelength might be due to internal device heating as a result of the higher  $I/I_{th}$  ratio in the annealed lasers.

In order to calculate the values of  $dg/dn$  and  $\varepsilon$ , the internal quantum efficiency ( $\eta_i$ ) and internal loss ( $\alpha_i$ ) are determined by measuring the as-grown and annealed lasers with different cavity length (1–4 mm) at different temperatures [18], [19]. Fig. 2 shows the relationship between the reciprocal of external quantum efficiency ( $\eta_d$ ) and the cavity length  $L$  from a batch of as-cleaved as-grown and annealed lasers at 10 °C and 70 °C, respectively. At each temperature, the internal quantum efficiency  $\eta_i$  of the annealed lasers is higher than that of the as-grown ones, while  $\alpha_i$  is slightly smaller, as compared with the as-grown ones. This could be attributed to the reduction in defect density in annealed QDs as reported in our previous work [14].

Small-signal modulations were carried out at different temperatures ( $T$ ) to study the effect of annealing on the high-speed properties of QD lasers. Fig. 3 shows the small-signal response curves for the as-grown lasers measured at (a) 10 °C and (b) 70 °C and annealed lasers measured at (c) 10 °C and (d) 70 °C. Fig. 4(a) and (b) show the lasing spectrum, measured at 70 °C, of the 1-mm-long as-grown and annealed lasers at 240 mA ( $2.23 I_{th}$ ) and 260 mA ( $3.63 I_{th}$ ), respectively. Notice that no ES lasing has been observed in the annealed lasers, while ES lasing starts to appear at high injection currents for the as-grown lasers. The bandwidth of the as-grown lasers is 8.2 GHz at 10 °C and 2.8 GHz at 70 °C, while the bandwidth for the annealed lasers is 8.5 GHz at 10 °C and 5.3 GHz at 70 °C. As such, the bandwidth of the as-grown lasers is more sensitive to the temperature, as compared with the annealed ones. The small-signal response curves were fitted

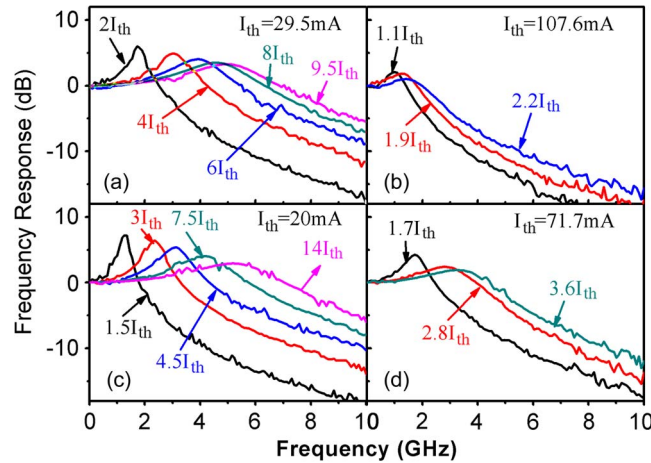


Fig. 3. Frequency response curves for the as-grown lasers measured at (a) 10 °C and (b) 70 °C and annealed lasers measured at (c) 10 °C and (d) 70 °C.

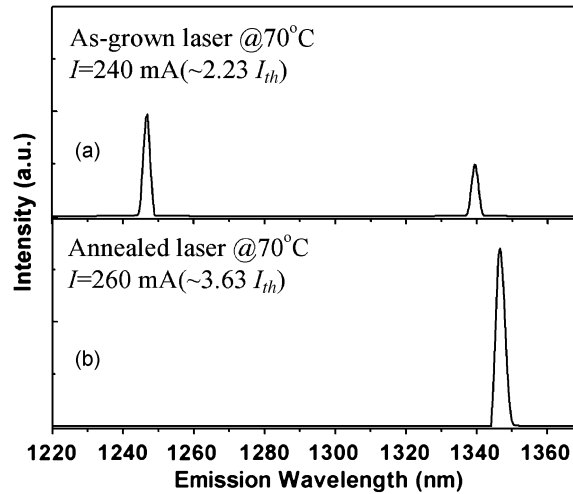


Fig. 4. Emission wavelength of the (a) as-grown and (b) annealed lasers at the corresponding injection currents at 70 °C.

with the modulation transfer function to extract the values of the damping rate  $\gamma$  and resonance frequency  $f_r$  at different bias currents [20], [21]

$$M(f) \propto \frac{f_r^4}{(f_r^2 - f^2)^2 + \frac{f^2}{4\pi^2} \gamma^2} \tag{1}$$

According to the plot of  $f_r$  versus the square root of the normalized bias current  $(I - I_{th})^{1/2}$ , the slope (known as the  $D$ -factor or modulation efficiency) is obtained, from which the value of differential gain ( $dg/dn$ ) is deduced. The relationship between  $f_r$  and  $\gamma$  defines the  $K$ -factor, which is used to determine the value of nonlinear gain compression factor ( $\epsilon$ ).

With the values of the temperature-dependent  $\eta_i$  and  $\alpha_i$ , the values of the temperature-dependent differential gain are obtained and plotted in Fig. 5. The improvement in  $dg/dn$  upon annealing might be due to an effective reduction in the carrier transportation time at the barriers and carrier capture and relaxation time into the QDs [9]. While the trend of decreasing  $dg/dn$  with increasing temperature is expected, notice that the degradation of  $dg/dn$  with temperature is almost doubled

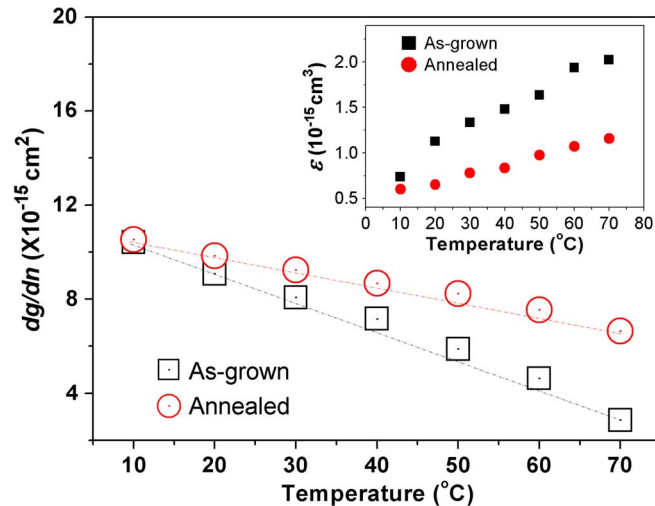


Fig. 5. Temperature dependence of differential gain for the as-grown and annealed lasers. Inset shows the temperature dependency of nonlinear gain compression for the as-grown and annealed lasers.

for the as-grown lasers, as compared with the annealed ones. Since the bandwidth is proportional to  $(dg/dn)^{0.5}$  [21], the high-speed performance of the annealed lasers is expected to exhibit better temperature stability, as compared with the as-grown ones. The temperature dependency of the nonlinear gain compression factor  $\epsilon$  is shown in the inset of Fig. 5. Similarly, one notices an improvement in the temperature stability since the increase in  $\epsilon$  with respect to temperature (i.e.,  $d\epsilon/dT$ ) for the annealed lasers is only halved of that of the as-grown ones. The gain compression in QDs is affected by the time needed to re-establish the intraband steady-state populations, which in turn is limited by the electron relaxation time of the InAs/GaAs system [3]. Hence, the smaller values of  $\epsilon$  in the annealed QDs might be due to faster electron-relaxation time. More importantly, since gain compression limits the bandwidth of QD lasers by affecting the  $K$ -factor [21], smaller  $\epsilon$  at higher temperature thus translate to larger bandwidth of the annealed lasers, as compared with the as-grown ones. Differential gain and gain compression have been shown to be limited by intradot relaxation in the conduction band [3]. Therefore, higher differential gain and lower gain compression, as exhibited by the annealed QDs laser, are possibly due to faster electron relaxation.

The carrier dynamics are important in determining the high-speed performance of the QD lasers and the observed improvement in the dynamic characteristics of the annealed lasers, as compared with the as-grown ones (more obvious at higher temperature), might be due to more efficient carrier relaxation from ES to GS upon annealing. Note that the mechanism where carriers relax from the barrier into the QDs first involves carriers being captured into ES, followed by relaxation from ES to GS. Similar capture-time-limited-bandwidth at high temperature has been reported by Klotzkin *et al.* [22], and it was found that the capture of electrons is more critical since its capture rate is slower than that of the holes. However, it was also found that the time required for the carriers to be captured from the barrier layer to the ES of QDs is faster than that required to GS [23]. Since ES has been suppressed in the annealed lasers (as shown in Fig. 4), the carrier relaxation time from ES to GS is believed to be shorter for the annealed QDs [14]. It was recently reported that an improvement of  $\sim 1$  GHz in the bandwidth can be expected from a 1-ps reduction in the relaxation time [4]. Hence, the observed increase in the bandwidth of 0.3 GHz and 1.5 GHz at 10 °C and 70 °C, respectively, from the annealed QDs might possibly be due to a reduction in the relaxation time on the order of 0.1 ps.

#### 4. Conclusion

In summary, we investigated the effect of RTA on thermal stability of dynamic characteristics of QD lasers. The characteristic temperature has been enhanced by a factor of 2.3 upon annealing. ES lasing has been suppressed after RTA process, and the carrier capture and relaxation to GS

may have been enhanced after RTA. The differential gain has been increased, and nonlinear gain compression has been reduced in the annealed QD laser. More importantly, the temperature stability of these two parameters has been improved after RTA. This shows that the RTA process could improve the dynamic characteristics of InAs/GaAs QD lasers, which is important for the development of uncooled high-speed QD lasers.

## Acknowledgment

The authors gratefully acknowledge the support of Dr. D. R. Lim, Dr. V. Wong, X. Guo, F. W. Lor, and Dr. E. K. Lee.

## References

- [1] O. B. Shchekin and D. G. Deppe, "The role of  $p$ -type doping and the density of states on the modulation response of quantum dot lasers," *Appl. Phys. Lett.*, vol. 80, no. 15, pp. 2758–2760, Apr. 2002.
- [2] D. Klotzkin, K. Kamath, K. Vineberg, P. Bhattacharya, R. Murty, and J. Laskar, "Enhanced modulation bandwidth (20 GHz) of  $\text{In}_{0.4}\text{Ga}_{0.6}\text{As}$ -GaAs self-organized quantum-dot lasers at cryogenic temperatures: Role of carrier relaxation and differential gain," *IEEE Photon. Technol. Lett.*, vol. 10, no. 7, pp. 932–934, Jul. 1998.
- [3] A. Fiore and A. Markus, "Differential gain and gain compression in quantum-dot lasers," *IEEE J. Quantum Electron.*, vol. 43, no. 4, pp. 287–294, Apr. 2007.
- [4] C. Z. Tong, D. W. Xu, and S. F. Yoon, "Carrier relaxation and modulation response of 1.3- $\mu\text{m}$  InAsGaAs quantum dot lasers," *J. Lightw. Technol.*, vol. 27, no. 23, pp. 5442–5450, Dec. 2009.
- [5] S. Fathpour, Z. Mi, and P. Bhattacharya, "Small-signal modulation characteristics of  $p$ -doped 1.1- and 1.3- $\mu\text{m}$  quantum-dot lasers," *IEEE Photon. Technol. Lett.*, vol. 17, no. 11, pp. 2250–2252, Nov. 2005.
- [6] D. G. Deppe and D. L. Huffaker, "Quantum dimensionality, entropy, and the modulation response of quantum dot lasers," *Appl. Phys. Lett.*, vol. 77, no. 21, pp. 3325–3327, Nov. 2000.
- [7] D. G. Deppe, H. Huang, and O. B. Shchekin, "Modulation characteristics of quantum-dot lasers: The influence of  $p$ -type doping and the electronic density of states on obtaining high speed," *IEEE J. Quantum Electron.*, vol. 38, no. 12, pp. 1587–1593, Dec. 2002.
- [8] H. S. Djie, Y. Wang, B. S. Ooi, D. N. Wang, J. C. M. Hwang, G. T. Dang, and W. H. Chang, "Defect annealing of InAs-InAlGaAs quantum-dash-in-asymmetric-well laser," *IEEE Photon. Technol. Lett.*, vol. 18, no. 22, pp. 2329–2331, Nov./Dec. 2006.
- [9] S. Marcinkevicius and R. Leon, "Carrier capture and escape in  $\text{In}_x\text{Ga}_{1-x}\text{As}$ /GaAs quantum dots: Effects of intermixing," *Phys. Rev. B, Condens. Matter*, vol. 59, no. 7, pp. 4630–4633, Feb. 1999.
- [10] S. Malik, E. C. Le Ru, D. Childs, and R. Murray, "Time-resolved studies of annealed InAs/GaAs self-assembled quantum dots," *Phys. Rev. B, Condens. Matter*, vol. 63, no. 15, pp. 1–6, Apr. 2001.
- [11] H. S. Djie, Y. Wang, D. Negro, and B. S. Ooi, "Postgrowth band gap trimming of InAs/InAlGaAs quantum-dash laser," *Appl. Phys. Lett.*, vol. 90, no. 3, pp. 031 101-1–031 101-3, Jan. 2007.
- [12] Z. Y. Zhang, Q. Jiang, and R. A. Hogg, "Tunable interband and intersubband transitions in modulation C-doped InGaAs/GaAs quantum dot lasers by postgrowth annealing process," *Appl. Phys. Lett.*, vol. 93, no. 7, p. 071 111, 2008.
- [13] R. Wang, C. Z. Tong, S. F. Yoon, C. Y. Liu, H. X. Zhao, and Q. Cao, "Temperature characteristics of gain profiles in 1.3  $\mu\text{m}$   $p$ -doped and undoped InAs/GaAs quantum dot lasers," *IEEE Electron. Device Lett.*, vol. 30, no. 12, pp. 1311–1313, Dec. 2009.
- [14] Q. Cao, S. F. Yoon, C. Z. Tong, C. Y. Ngo, C. Y. Liu, R. Wang, and H. X. Zhao, "Two-state competition in 1.3- $\mu\text{m}$  multilayer InAs/InGaAs quantum dot lasers," *Appl. Phys. Lett.*, vol. 95, no. 19, pp. 191 101-1–191 101-3, Nov. 2009.
- [15] Q. Cao, S. F. Yoon, C. Y. Liu, and C. Z. Tong, "Effects of rapid thermal annealing on optical properties of  $p$ -doped and undoped InAs/InGaAs dots-in-a-well structures," *J. Appl. Phys.*, vol. 104, no. 3, pp. 033 522-1–033 522-6, Aug. 2008.
- [16] S. Sanguinetti, T. Mano, A. Gerosa, C. Somaschini, S. Bietti, N. Koguchi, E. Grilli, M. Guzzi, M. Gurioli, and M. Abbarchi, "Rapid thermal annealing effects on self-assembled quantum dot and quantum ring structures," *J. Appl. Phys.*, vol. 104, no. 11, pp. 113 519-1–113 519-5, Dec. 2008.
- [17] J. Tatebayashi, Y. Arakawa, N. Hatori, H. Ebe, M. Sugawara, H. Sudo, and A. Kuramata, "InAs/GaAs self-assembled quantum-dot lasers grown by metalorganic chemical vapor deposition—Effects of postgrowth annealing on stacked InAs quantum dots," *Appl. Phys. Lett.*, vol. 85, no. 6, pp. 1024–1026, Aug. 2004.
- [18] C. Y. Liu, S. F. Yoon, Q. Cao, C. Z. Tong, and H. F. Li, "Low transparency current density and high temperature operation from ten-layer  $p$ -doped 1.3  $\mu\text{m}$  InAs/InGaAs/GaAs quantum dot lasers," *Appl. Phys. Lett.*, vol. 90, no. 4, p. 041 103, Jan. 2007.
- [19] L. V. Asryan, "Limitations on standard procedure of determining internal loss and efficiency in quantum dot lasers," *J. Appl. Phys.*, vol. 99, no. 1, pp. 013 102-1–013 102-4, Jan. 2006.
- [20] M. Sugawara, N. Hatori, M. Ishida, H. Ebe, and Y. Arakawa, "Recent progress in self-assembled quantum-dot optical devices for optical telecommunication: Temperature-insensitive 10 Gbs<sup>-1</sup> directly modulated lasers and 40 Gbs<sup>-1</sup> signal-regenerative amplifiers," *J. Phys. D, Appl. Phys.*, vol. 38, no. 13, pp. 2126–2134, Jul. 2005.
- [21] L. A. Coldren and S. W. Corzine, *Diode Lasers and Photonic Integrated Circuits*. Hoboken, NJ: Wiley, 1995.
- [22] D. Klotzkin and P. Bhattacharya, "Temperature dependence of dynamic and DC characteristics of quantum-well and quantum-dot lasers: A comparative study," *J. Lightw. Technol.*, vol. 17, no. 9, pp. 1634–1642, Sep. 1999.
- [23] T. R. Nielsen, P. Gartner, and F. Jahnke, "Many-body theory of carrier capture and relaxation in semiconductor quantum-dot lasers," *Phys. Rev. B, Condens. Matter*, vol. 69, no. 23, pp. 235 314-1–235 314-13, Jun. 2004.